Supplementary Information:

Enhanced Spatial Mapping of Histone Proteoforms in Human Kidney Through MALDI-MSI by High-Field UHMR Orbitrap Detection

Kevin J. Zemaitis,[1] Dušan Veličković,[1] William Kew,[1] Kyle L. Fort,[2] Maria Reinhardt-Szyba,[2] Annapurna Pamreddy,[3] Yanli Ding,[4] Dharam Kaushik,[5] Kumar Sharma,[3, 6] Alexander A. Makarov,[2, 7] Mowei Zhou,[1] and Ljiljana Paša-Tolić[1,*]

[1] Environmental Molecular Sciences Laboratory, Pacific Northwest National Laboratory, Richland, Washington 99352, United States

[2] Thermo Fisher Scientific (Bremen) GmbH, 28199 Bremen, Germany

[3] Center for Renal Precision Medicine, Department of Medicine, University of Texas Health, San Antonio, Texas 78284, United States

[4] Department of Pathology and Laboratory Medicine, University of Texas Health, San Antonio, Texas 78284, United States

[5] Department of Urology, University of Texas Health, San Antonio, Texas 78284, United States

[6] Audie L. Murphy Memorial VA Hospital, South Texas Veterans Health Care System, San Antonio, Texas 78284, United States

[7] Biomolecular Mass Spectrometry and Proteomics, Bijvoet Center for Biomolecular Research and Utrecht Institute for Pharmaceutical Sciences, University of Utrecht, Utrecht 3584, The Netherlands

Corresponding Author**:**

* Ljiljana Paša-Tolić – Email: ljiljana.pasatolic@pnnl.gov

Contents:

Extended Instrumental Parameters:

The EP-MALDI source from Spectroglyph, LLC is equipped with a 2000 Hz Explorer One (349 nm) laser (Spectra Physics, Stahnsdorf, Germany).[1] The dual ion funnel source RF was initially autotuned and amplitude (V_{p-p}) adjusted with standards to optimize transmission. No alterations were made to the EP-MALDI source at this time. If not noted, default parameters provided by the manufacturer at installation were utilized for settings of the ion optics. The high-pressure funnel pressure was manually regulated to 6.1 Torr, the fore vacuum of the MS was regulated at 1.25 mbar, and the ultrahigh vacuum was measured at an average of 2.5e-10 mbar with UHP nitrogen trapping gas. Argon was also evaluated with minor visible changes in results, HCD performance was not evaluated within this study. It was found that for certain matrixes and sample preparation operating the dual ion funnel source on the order of 150-250 V_{p-p} aided in breaking up matrix clusters on larger proteins. This is exemplified within dried droplet preparations.

Laser conditions were optimized on tissue as to not oversample and not burn through the tissue, resulting in a repetition rate set to 500 Hz with the diode set to deliver an average of 1.0 to 1.1 µJ per pulse as measured through the software. Lasing was continuous and stage movements were synchronized through an instrument trigger signal. A fixed ion injection time of 500 ms resulted in 250 laser shots per pixel, with a 0.512 second transient resulting in an acquisition rate of 0.512 seconds per pixel, or 2 Hz. The laser beam was focused to approximately 12 by 15 µm, and the pixel size was set to either 20 or 30 µm, as stated within the Figures. The laser beam size was measured through calculation of the desorption crater through light microscopy. The upgraded UHMR Q Exactive HF has several ion transfer settings which also required optimization, but many default values for ion transfer for 'high *m/z'* were found to be sufficient with detector *m/z* optimization also set to 'high *m/z'*. Further manual tuning had minimal gains; however, each parameter should be evaluated on new tissue types including all relevant DC potentials in the MALDI source and the injection flatapole DC, inter flatapole lens, and bent flatapole DC. Trapping gas pressure was set to 1.2 for these experiments with nitrogen gas.

Exemplary spectra of CsI clusters created by direct infusion ESI exemplify the detection bias which can be created through the tuning of the ion transfer and detector settings for default 'low *m/z*' and default 'high *m/z*' settings. This is shown within Supplementary Figure S2, and furthermore it was found that increasing the low mass for detection increased the abundance of higher mass proteins. Shown in Supplementary Figure S4 is the result on on-tissue optimization of IST, this concept is explained within literature,[2] however it was found for implementation of MALDI it was necessary for detection of intact proteins. Interestingly, there are three tunable parameters for IST, it was found that desolvation time (4-10 ms) and trapping voltage (± 60 V) had minimal effects on protein signal. The most influence came from tuning of the desolvation voltage (± 300 V). This suggests that IST also plays a large role within breaking of matrix clusters, similar to in-source fragmentation which can be noted within small molecules by operating the dual funnel at increased levels of V_{p-p} (>150-250 V_{p-p}), which in the case of MALDI was also found to be beneficial. Overall, the parameter space was found to be very robust for this imaging platform.

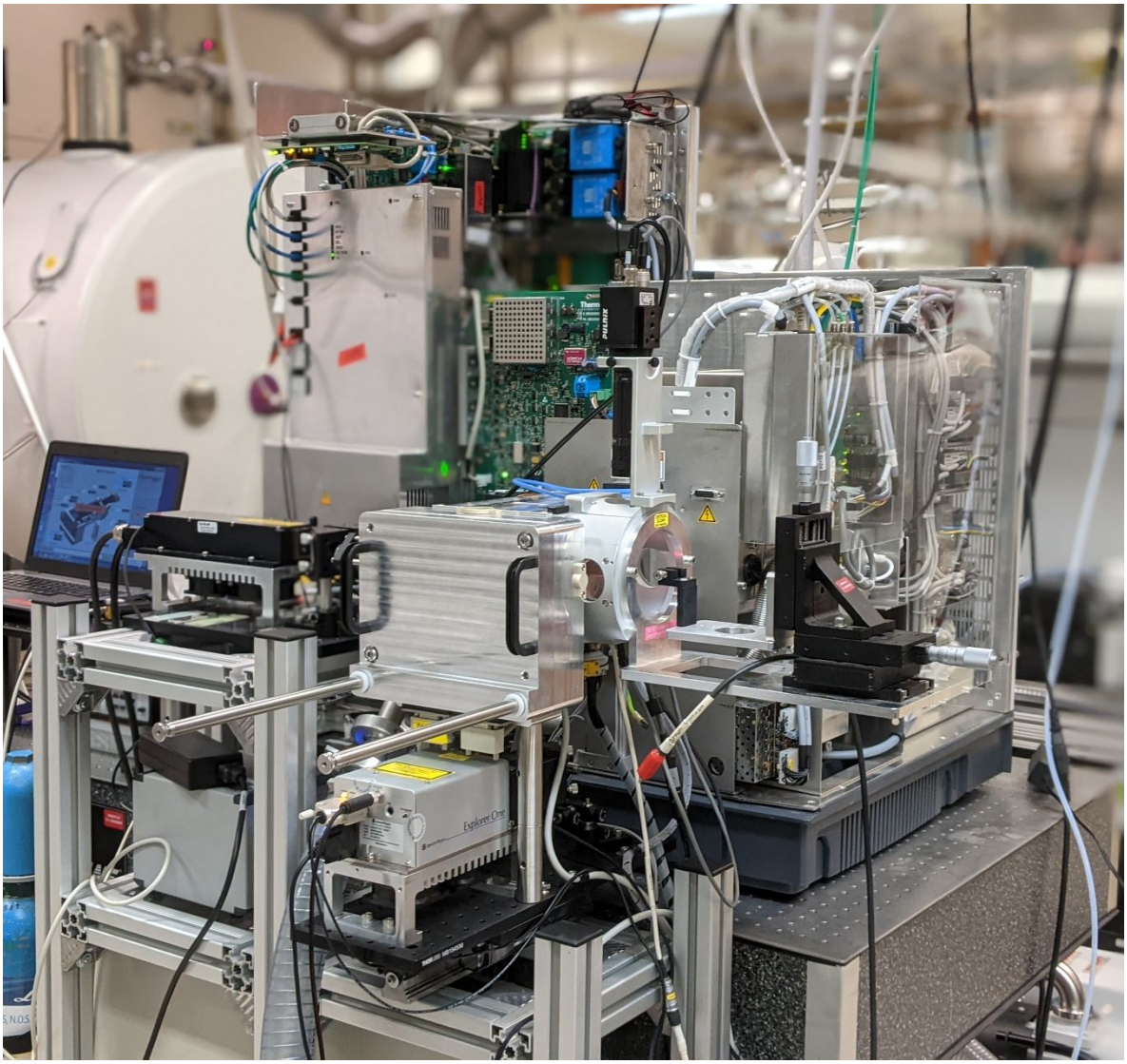

Supplementary Figure S1: Digital photograph of the Spectroglyph EP-MALDI source mounted on the upgraded UHMR Q Exactive HF, pictured with a nanospray source mounted. The UHMR Q Exactive HF fitted with the MALDI source was found to still produce similar results for native static nanospray MS experiments, and the HESI source was alternatively mounted for calibration of the MS.

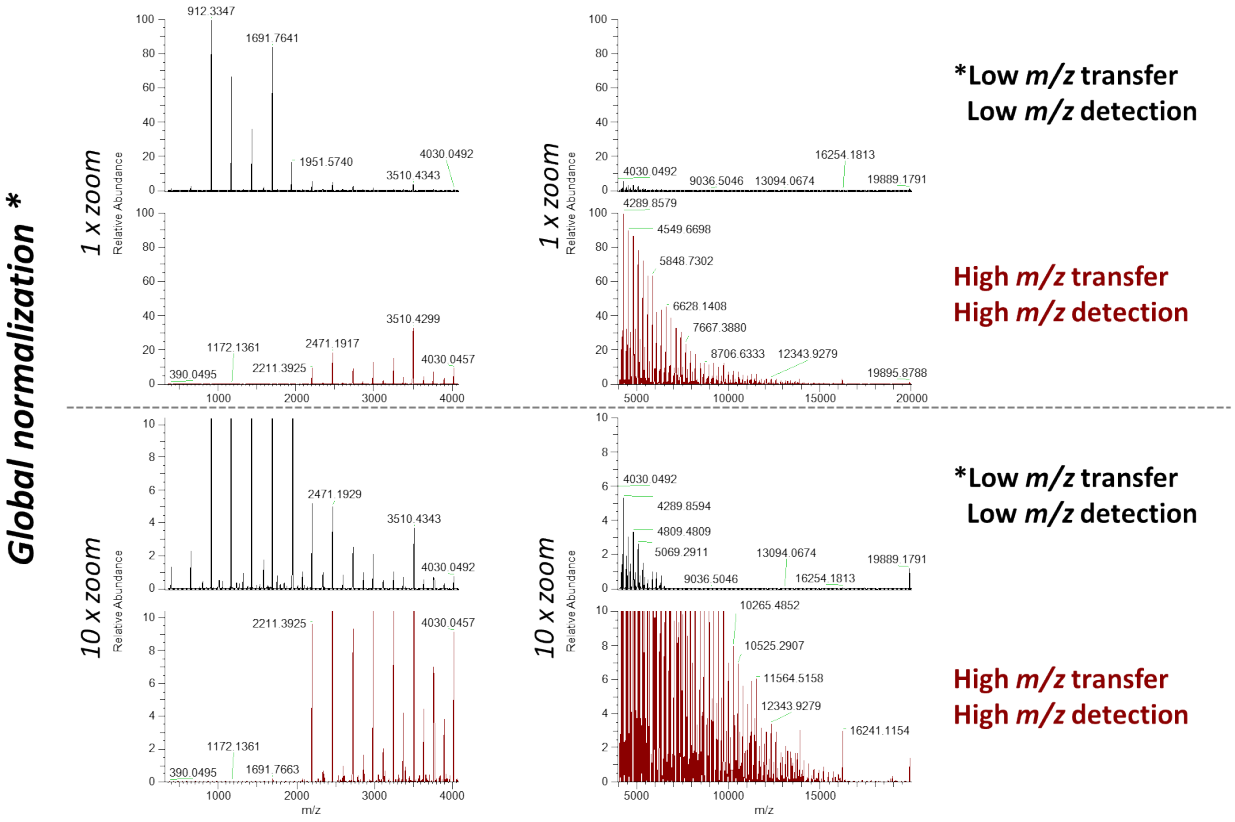

Supplementary Figure S2: Exemplary spectra of calibration spectra using CsI sprayed at 2 mg/mL in 50% isopropanol for the default ion transfer and detector settings for both 'high *m/z*' and 'low *m/z*'. This demonstrates the effects seen within the default tuning on expected mass ranges, where a high mass bias is observed within 'high *m/z*' modes and low mass bias is observed in 'low *m/z*' modes for ion transfer and detection settings. Within 'low *m/z*' operation the UHMR Q Exactive HF operates similar to a standard Q Exactive HF but with a restricted low mass of 350 and signal is observed beyond *m/z* 6000, however, the signal is severely attenuated. A comparison of signal intensity was not completed when the instrument was a standard Q Exactive HF.

With operation in high mass modes, switched to 'high *m/z*' default parameters signal below *m/z* 2000 is found to be attenuated in comparison, however, the usable mass range is now extended to the largest CsI clusters at > *m/z* 15000. Signal for CsI shows higher intensity starting at *m/z* 2211.3925 as demonstrated in the inset 10 times zoom panel. Therefore, for some MALDI analyses of glycans, peptides, and/or proteins it can be recommended to complete separate imaging analyses for the best results or complete manual tuning.

These effects are also similar to mass biases which can be noted from decreased or increased TOF within broadband measurements made by FTICR. The spectra are globally normalized to the highest intensity in the spectrum indicated by an asterisk (*) within Freestyle (v.1.8 SP1).

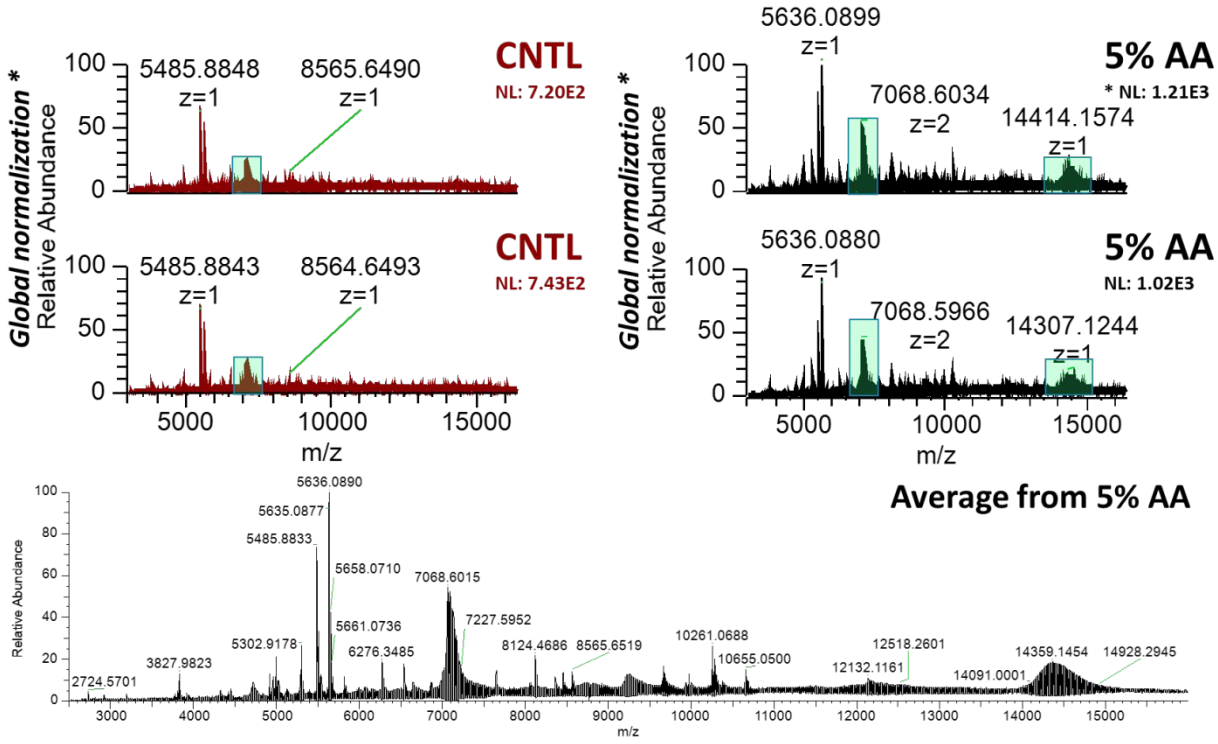

Supplementary Figure S3: Each inset spectrum represents an average of equivalent number of acquisitions corresponding to serial line scans within a coronal section of Sprague Dawley rat brain cryo-sectioned at 12 µm. For the purposes of these experiments, the same instrumental and source parameters were used, and the brains were coated in matrix at the same time. (CNTL) underwent no tissue acidification and (5% AA) underwent tissue acidification through the spraying of 5% acetic acid (*v/v*) in 50% ethanol via an HTX M5 Sprayer as outlined within methods. Shown within the inset figures are technical replicates, which correspond to an additional serial line scan for each treatment. The spectra are globally normalized within Freestyle (v.1.8 SP1) to the highest intensity line scan indicated by an asterisk (*). Histone H2A proteoforms are highlighted within each spectrum, these were the most prominent core histone proteoforms within this region of rat brain and can be observed as a doubly charged cluster centered at *m/z* 7070 and singly charged cluster at *m/z* 14140. Several other distinct species also can be noted as enhanced through this sample pretreatment as well (i.e., *m/z* 5636). An average spectrum of 2000 scans from the 5% AA treatment is shown on the bottom. Within this spectrum, it can also be observed the histone H2A cluster overlaps with other protein envelopes (e.g., myelin basic protein). Regardless of this fact, this demonstrates a significant enhancement of signal (e.g., a 2-fold increase for histone H2A proteoforms) after sample pretreatment vs. control. This data also suggest enhancement of histone signal through this additional sample preparation step is likely not tissue type specific.

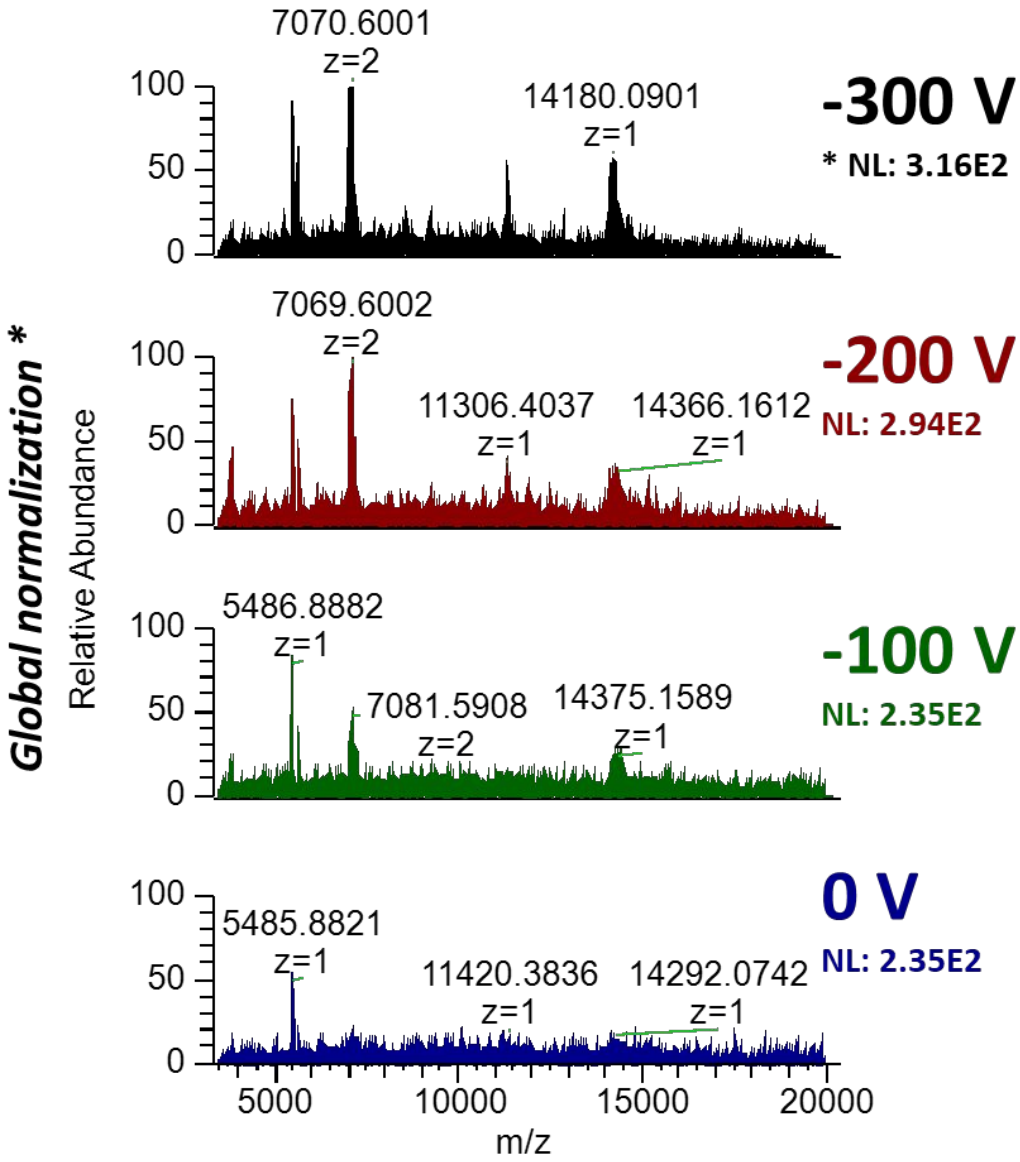

Supplementary Figure S4: Exemplary spectra from the tuning of the desolvation voltage for IST,[2] where voltages were profiled at -25 V intervals and were tested on serial line scans from a rectangular measurement area on portion of human kidney prepared utilizing the outline protocol in the Experimental section of the main text. The top inset figure shows the average of 36 scans with a desolvation volage of -300 V. Where each subsequent inset spectrum corresponds to the same number of averages in serial line scans, each is labelled with the subsequent desolvation voltage used in positive ion mode. Four exemplary spectra are shown, including desolvation voltages of 0 V, -100 V, -200 V, and -300 V. The doubly charged cluster centered at *m/z* 7070 and singly charged cluster at *m/z* 14100, corresponds to histone H2A proteoforms, these are shown to gain significant intensity at higher desolvation voltages. Similarly, the other smaller peptides detected, as well as the singly charged histone H4 cluster starting at *m/z* 11306 have similar responses. Desolvation time and trapping voltages were not found to have as profound of an effect but should be evaluated within the tuning and optimization of different sample preparations and on different tissue types. The spectra are globally normalized to the highest intensity in the spectrum indicated by an asterisk (*) within Freestyle (v.1.8 SP1).

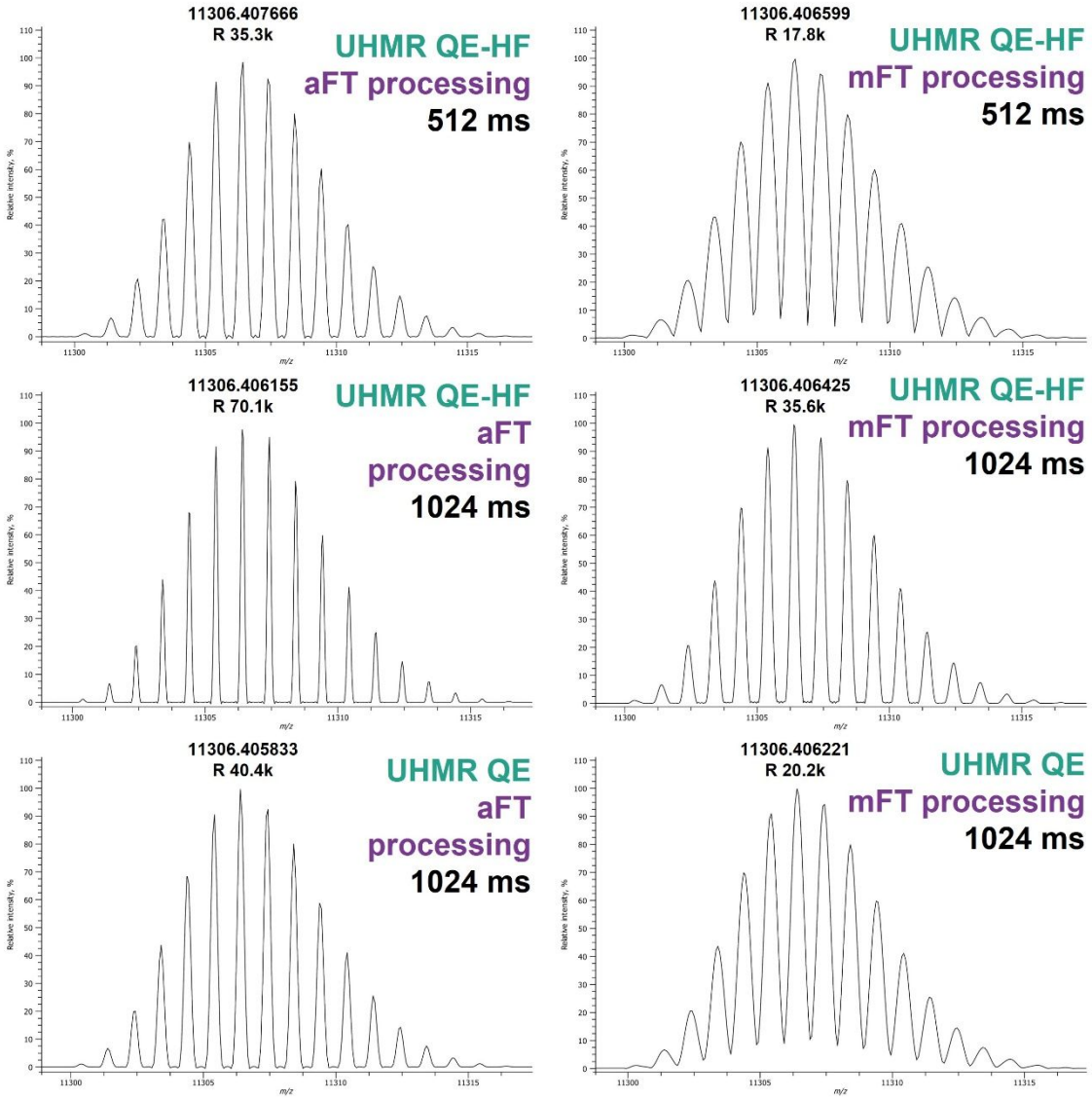

Supplementary Figure S5: Utilizing the isotopic distribution simulator within Peak-by-Peak software by Spectroswiss,[3] a comparison between maximum transient lengths used for the commercial UHMR Q Exactive (1024 ms), and this custom UHMR Q Exactive HF (512 and 1024 ms) was completed. Simulated patterns for both magnitude (mFT) and absorption mode (aFT) processing were completed utilizing all default settings for a protonated human histone H4 N-Ac K20me2 without noise and decay added. It should be noted that Orbitrap MS platforms utilize an enhanced Fourier transform (eFT), which was experimentally found to be equivalent to aFT results, and provides at least a 1.4-fold enhancement per literature report.[4] It should also be noted that actual eFT vs. mFT experimental measurements on Orbitrap MS will double the length of the transient to maintain resolving power if eFT is disabled when a preset resolution is set (i.e., 240k at *m/z* 200). On a Q Exactive HF, this would correspond to 0.512 second transient for eFT and if eFT is disabled and the MS would acquire a 1.024 second transient. Thus, aFT vs. mFT simulations shown above are not what occur experimentally; however, they are accurate for common transient lengths and duty cycles for different processing. Results shown above for the UHMR Q Exactive and UHMR Q Exactive HF correspond to a 1 or 2 Hz duty cycle per pixel.

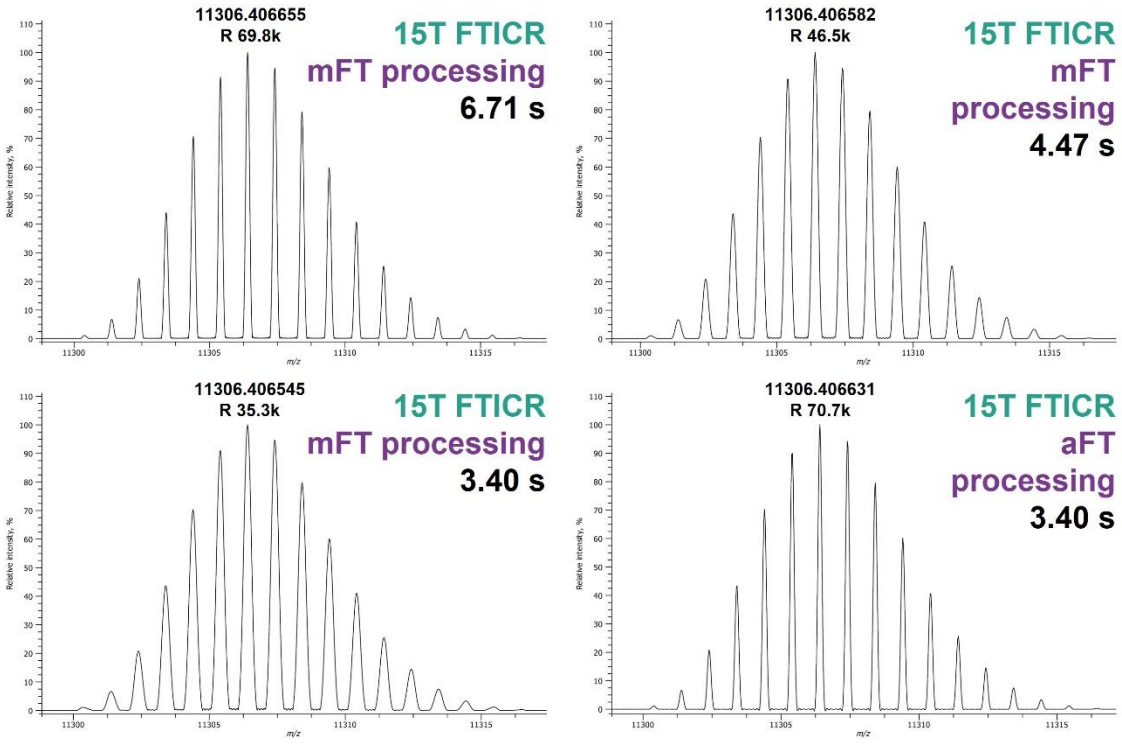

Supplementary Figure S6: Utilizing the isotopic distribution simulator within Peak-by-Peak software by Spectroswiss,[3] a comparison between commonly reported transient lengths used for commercial 15T FTICR for intact protein MALDI-MSI was completed.[5, 6] Simulated patterns for both magnitude (mFT) and absorption mode (aFT) processing were completed utilizing all default settings for a protonated human histone H4 N-Ac K20me2 without noise and decay added. This was completed to properly compare FTICR MSI to UHMR Q Exactive HF MSI with the denoted base peak within this analysis. It should be noted that aFT processing for MALDI-FTICR-MSI datasets has been demonstrated through proof of principle and applied studies but is only commonly implemented for routine small molecules, metabolites, and lipids imaging (despite potentially doubling the expected resolution per duty cycle) and other analyses. It should also be noted that to the authors knowledge there has been no literature report of intact protein MALDI-MSI using aFT processing or frequency multiple detection within extended mass ranges, and a vast majority of aFT reports have not demonstrated the full theoretical improvement from aFT. Experimentally simulated mFT processing of a 3.40 s transient is comparable to eFT processing of UHMR Q Exactive HF datasets.

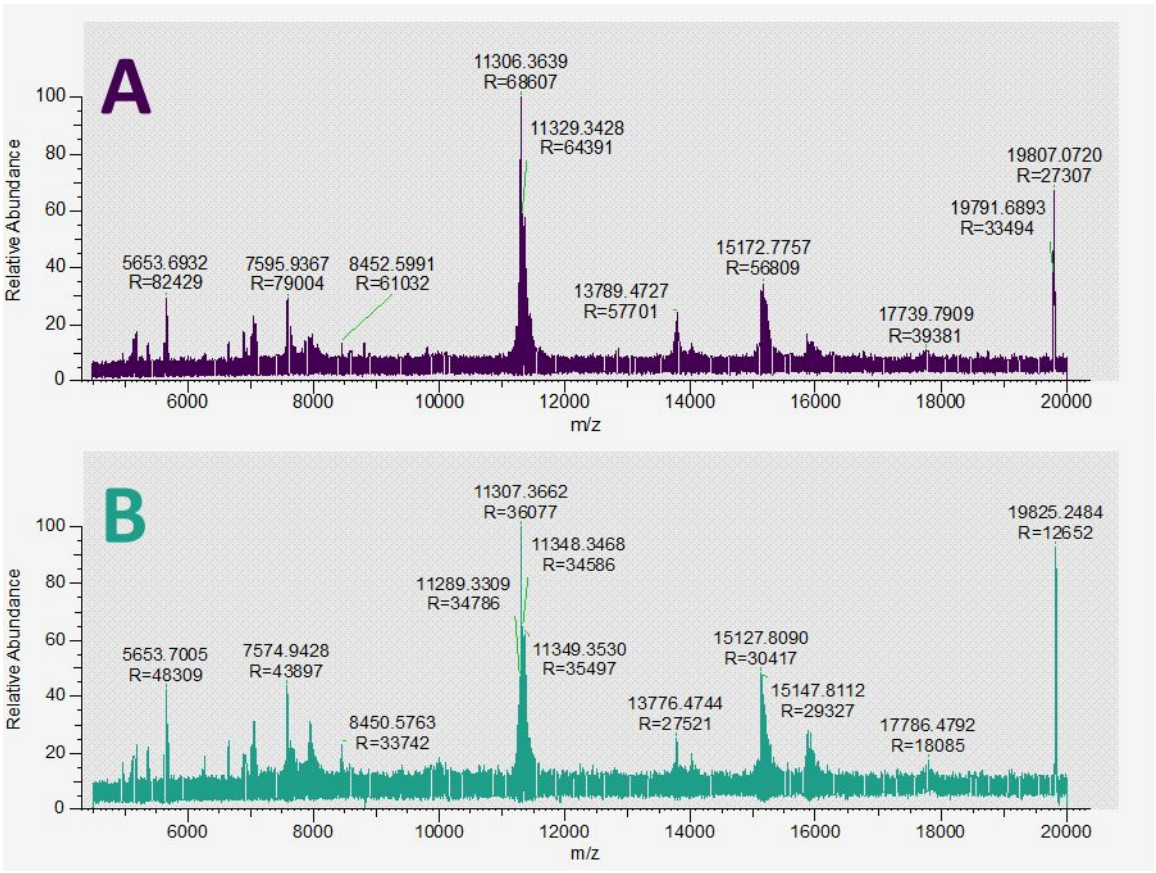

Supplementary Figure S7: An average of 50 acquisitions corresponding to line scans at set resolution of (A) "480k" at *m/z* 200 matching a transient time of 1.024 s, and (B) "240k" at *m/z* 200 matching a transient time of 0.512 second on the UHMR Q Exactive HF. The effective duty cycle for acquisition speed results in 1 Hz and 2 Hz scan rates; this is due to ion accumulation periods (fixed at 500 ms) being less than detection periods and the Orbitrap MS performing parallel accumulation during detection. The observed resolution at *m/z* 11307 is 68.6k for (A) and 36.0k for (B) corresponds to an improvement of 1.9-fold for double the transient length. Through the detected *m/z* range of $4500 < m/z < 20000$, mass resolution improvement (at FWHM) varies from a 1.7-fold to 1.9-fold, with the average improvement of 85% of the full theoretical 2-fold enhancement for doubling the transient length after averaged several dozen scans.

The theoretical simulation of isotopic distributions and resolution of the base peak in each of these spectra, which is annotated as protonated histone H4 N-ac K20me2, is shown in Fig. S3 for 240k measurements for (A). These same simulations of the base peak isotopic distributions and theoretical resolutions are located within Fig. S3 for 480k measurements for (B). Comparison of these experimental observations and theoretical aFT simulations show slight signal decay within the extended 1.024 second transient, while observed eFT resolutions are equivalent to full theoretical aFT processing for 0.512 second transients. The spectra are plotted within Freestyle (v.1.8 SP1).

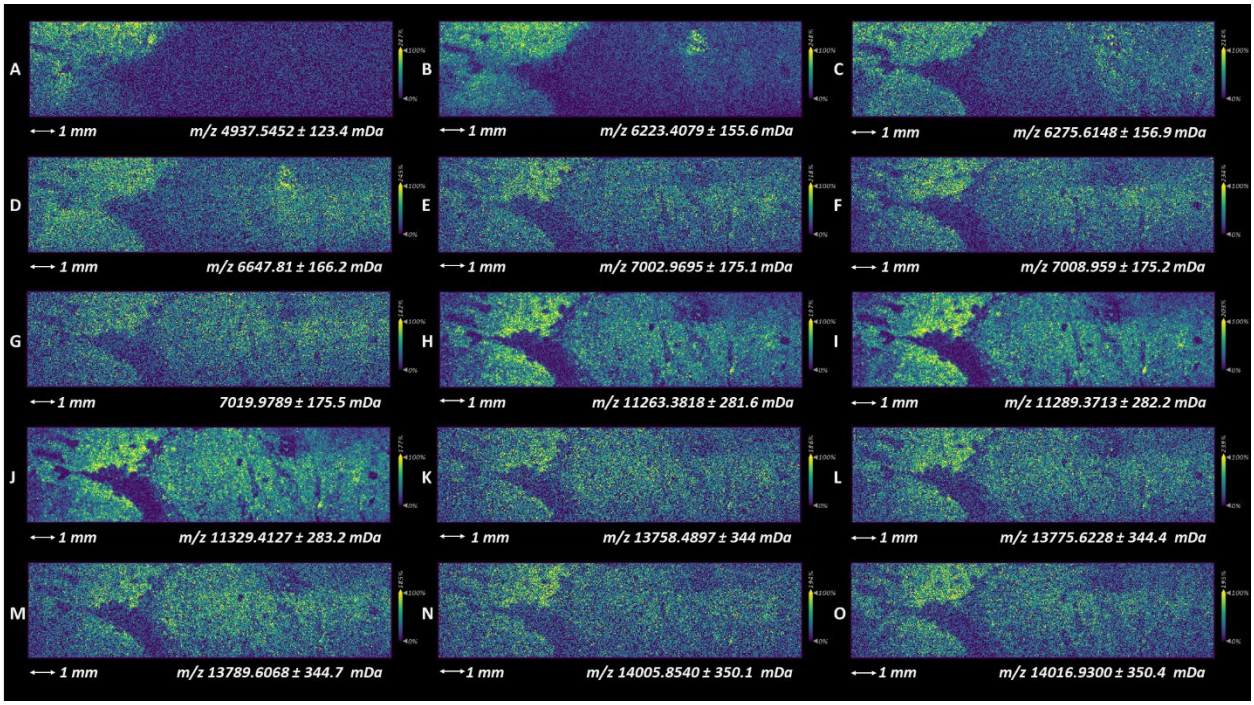

Supplementary Figure S8: Additional proteoform images from the tubular atrophy nephrectomy section including several distributions of small proteins (A, B, C, and D) which include annotations such as 40S ribosomal protein 30S (D), as well as various proteoforms of histones H4, H2A, and H2B (E, F, and G are doubly charged, where H through O are singly charged).

Instrument	FT Processing	Transient (FID)	Resolution at *m/z* 11306
UHMR Q Exactive	mFT	1.024 s	20.2k
UHMR Q Exactive	aFT	1.024 s	40.4k
UHMR Q Exactive HF	mFT	512 ms	17.8k
UHMR Q Exactive HF	**aFT**	**512 ms**	**35.3k**
UHMR Q Exactive HF	mFT	1.024 s	35.6k
UHMR Q Exactive HF	**aFT**	**1.024 s**	**70.1k**
15T FTICR	**aFT**	**3.40 s**	**70.7k**
15T FTICR	**mFT**	**3.40 s**	**35.3k**
15T FTICR	mFT	4.47 s	46.5k
15T FTICR	**mFT**	**6.71 s**	**69.8k**

Table S1: Extracted resolution from the simulations performed in Peak-by-Peak software by Spectroswiss for the A+6 isotopologue of the protonated histone H4 N-Ac K20me2. FT processing is indicated as either magnitude (mFT) or absorption (aFT) for the listed transient lengths. Highlighted within teal and purple are comparisons between UHMR Q Exactive HF and 15T FTICR for similar resolution settings for both 35k resolution (purple) and 70k resolution (teal) at *m/z* 11,306. Note experimental eFT performance was nearly equivalent to aFT simulations. This represents a 6.6-fold increase in duty cycle comparing theoretical aFT processing of UHMR Q Exactive HF Orbitrap (which is equivalent to experimentally observed resolutions with eFT) to mFT processing of 15T FTICR MS. If both instruments were operated within mFT configurations, or if advanced aFT processing was completed on the 15T FTICR MS (orange) this would still represent a 3.3-fold improvement in resolution per unit time.

References:

1. Belov, M. E.; Ellis, S. R.; Dilillo, M.; Paine, M. R. L.; Danielson, W. F.; Anderson, G. A.; de Graaf, E. L.; Eijkel, G. B.; Heeren, R. M. A.; McDonnell, L. A., Design and Performance of a Novel Interface for Combined Matrix-Assisted Laser Desorption Ionization at Elevated Pressure and Electrospray Ionization with Orbitrap Mass Spectrometry. *Analytical Chemistry* **2017,** *89* (14), 7493-7501.
2. Fort, K. L.; van de Waterbeemd, M.; Boll, D.; Reinhardt-Szyba, M.; Belov, M. E.; Sasaki, E.; Zschoche, R.; Hilvert, D.; Makarov, A. A.; Heck, A. J. R., Expanding the structural analysis capabilities on an Orbitrap-based mass spectrometer for large macromolecular complexes. *Analyst* **2018,** *143* (1), 100-105.
3. Nagornov, K. O.; Kozhinov, A. N.; Gasilova, N.; Menin, L.; Tsybin, Y. O., Transient-Mediated Simulations of FTMS Isotopic Distributions and Mass Spectra to Guide Experiment Design and Data Analysis. *Journal of the American Society for Mass Spectrometry* **2020,** *31* (9), 1927-1942.
4. Lange, O.; Damoc, E.; Wieghaus, A.; Makarov, A., Enhanced Fourier transform for Orbitrap mass spectrometry. *International Journal of Mass Spectrometry* **2014,** *369*, 16-22.
5. Prentice, B. M.; Ryan, D. J.; Van de Plas, R.; Caprioli, R. M.; Spraggins, J. M., Enhanced Ion Transmission Efficiency up to m/ z 24 000 for MALDI Protein Imaging Mass Spectrometry. *Analytical chemistry* **2018,** *90* (8), 5090-5099.
6. Dilillo, M.; Ait-Belkacem, R.; Esteve, C.; Pellegrini, D.; Nicolardi, S.; Costa, M.; Vannini, E.; Graaf, E. L. d.; Caleo, M.; McDonnell, L. A., Ultra-High Mass Resolution MALDI Imaging Mass Spectrometry of Proteins and Metabolites in a Mouse Model of Glioblastoma. *Sci Rep* **2017,** *7* (1), 603-603.